Modelling installation of helical anchors in clay

C. Todeshkejoei & J.P. Hambleton
ARC Centre of Excellence for Geotechnical Science and Engineering, Centre for Geotechnical and Materials Modelling, The University of Newcastle, Callaghan, NSW, Australia

S.A. Stanier & C. Gaudin
ARC Centre of Excellence for Geotechnical Science and Engineering, Centre for Offshore Foundation Systems, The University of Western Australia, Crawley, WA, Australia

ABSTRACT: Helical anchors, which are mostly used to resist uplift, are deep foundations installed by rotation into the ground. Despite the central role of the installation process, especially with respect to the effect of soil disturbance, relatively little is known about the forces and deformations occurring during installation. An exception is the field verification technique known as torque-capacity correlation, which attempts to relate installation torque directly to uplift capacity. However, there are open questions regarding this approach, since not all significant parameters, such as installation vertical force and helix pitch, are taken into consideration. This could be one of the main reasons behind the wide range of torque-correlation factors reported in the literature. This study presents a three-dimensional numerical analysis of the installation process for helical anchors in clay. The results are synthesised into convenient yield envelopes that predict the relationship between installation torque and normal force as functions of helix pitch, roughness, and thickness. The application of the findings to torque-capacity correlation is also discussed.

1 INTRODUCTION

Helical anchors are screw-type foundations installed by rotating an assembly of helical plates attached to a central shaft into the ground (Figure 1). This type of foundation is most commonly used to resist uplift forces, although it can also be used in compression. The use of helical anchors has widely expanded both offshore and onshore during recent years due to the advantages of this system over traditional piles, which derive mainly from the method of installation. These advantages include cost effectiveness, capacity to resist loads immediately after installation, little or no vibration during installation, smaller crews and equipment, low weight of construction equipment, and ease of installation in all-weather conditions.

While numerous investigations have focused on predicting the uplift capacity of helical anchors (e.g., Merifield 2011, Wang et al. 2013), relatively few have considered the installation process, which not only determines the requirements for installation equipment but also influences anchor performance. The torque required for installation, denoted by T, depends on the properties of the soil, the configuration of the helical anchor, and the applied normal force, denoted by N. The combination of T and N dictates the rate at which the helical anchor advances into the soil, and this in turn affects the level of soil disturbance, an effect that existing theoretical approaches do not consider. On the other hand, the field verification method known as "torque-capacity correlation" rests on relating uplift capacity directly to the installation torque. This relationship is typically expressed as

$$N_u = KT \tag{1}$$

where N_u is the ultimate uplift capacity, K is the so-called torque correlation factor, and T is the installation torque, typically averaged over the last few revolutions during installation.

The majority of previous works on the installation process focus on torque-capacity correlation. One of the first studies was completed by Adams and Klym (1972), who performed field tests on dual-helix anchors in sand with embedment ratio H/D = 12.6, where H is the embedment depth and D is the plate diameter (Figure 1). Tsuha et al. (2007) and Tsuha and Aoki (2010) considered a range of configurations and embedment ratios based on physical modelling with sand. Weech (2002) performed six full-scale field tests on installation and uplift of helical anchors in lightly over-consolidated and highly sensitive fine-grained soil, allowing a recovery period following installation. Vyazmensky (2005) continued Weech's study and conducted one-dimensional numerical analyses to investigate pore pressure during installation. He studied time-dependent pore pressure response of the fine-grained soil caused by anchor installation. While all of the aforementioned studies focused on installation ef-

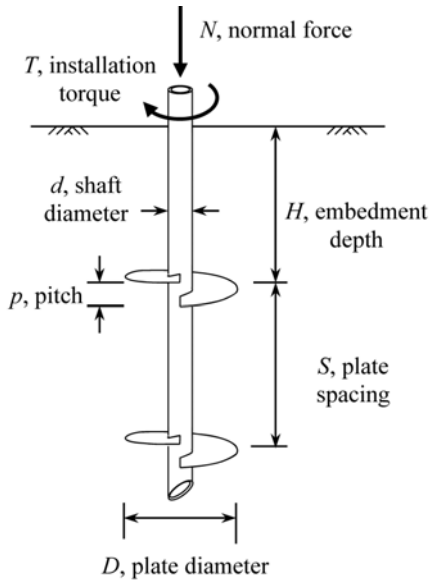

Figure 1. Schematic of helical anchor.

fects, none considered the effect of vertical force N and helix pitch p (Figure 1) on the installation torque T. The most relevant work on the installation process is the study by Perko (2000), who used energy equivalence theory to develop expressions for the torque correlation factor K. Perko concluded that K is (1) weakly dependent on final torque T, vertical force N and helix pitch p, (2) moderately affected by helix diameter D, and (3) strongly affected by shaft diameter d and helix thickness t.

This paper presents a new approach for modelling the installation of helical anchors in clay. Since the interaction between a helical anchor and soil during installation is incredibly complex, and modelling the true process of installation using conventional numerical techniques (e.g., finite element method) represents a significant challenge, this study introduces a simplified approach based on the analysis of an increment of deformation for a single, deeply embedded helix. The numerical results are presented in a series of envelopes relating installation torque T to normal force N for different values of pitch p, shaft diameter d, and helix thickness t. Expressions for the yield envelopes similar to those used to predict the capacity of plate anchors are developed, and the findings are subsequently interpreted in the context of the torque-capacity correlation method.

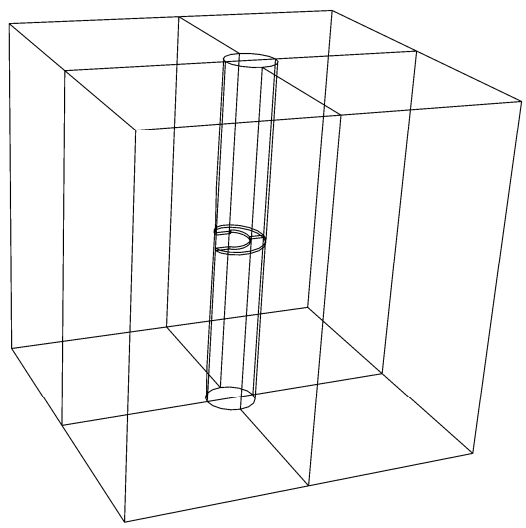

Figure 2. Example of finite element assembly (Case 9 from Table 1).

2 FINITE ELEMENT MODEL

The physical process by which helical anchors are installed from the ground surface involves large, plastic deformation, contact, and material separation. The full process therefore cannot be modelled using traditional finite element methods. In order to overcome this problem, it is assumed that the anchor has already penetrated to some depth within the soil, and the initial phase of installation when the helical anchor penetrates into the soil is neglected.

A parametric study based on small-strain finite element analysis was conducted using the commercial code ABAQUS. The analysis considered a single three-dimensional helix, and the effects of installation force, helix pitch, shaft and helix diameter, and helix thickness and roughness were investigated. An example of the full assembly from the finite element model is shown in Figure 2. The shaft itself was not represented due to high computational cost and difficulty in meshing, and the effect of the shaft diameter was considered only through its influence on the geometry of the helix. The helix was modelled as a rigid body, and the soil was discretised using tetrahedral quadratic modified elements. The element size in the vicinity of anchor was equal to the helix thickness. The soil was considered to be weightless, and elastoplastic analysis was performed assuming the Tresca yield criterion, with undrained shear strength denoted by s_u. The ratio of Young's modulus to undrained shear strength was set at $E/s_u = 500$, and the Poisson's ratio was kept equal to 0.49. The interaction between helices and soil was assumed to be either frictional, with friction coefficient μ, or fully rough, such that no relative sliding between the soil and helix was permitted. A single simulation was completed by first applying normal force N to the helix, and then rotating the helix until the reaction torque reached a roughly constant value corresponding to the installation torque T. Details of the finite element analyses are summarised in Table 1, which shows dimensions representative of industrial anchors.

Table 1. Details of all finite element analyses.

Case	D (m)	d (m)	t (m)	p (m)	Contact interaction
1		0			
2	1	0.2	0.05	0	Fully rough
3		0.4			
4		0			
5	1	0.2	0.05	0.16	Fully rough
6		0.4			
7		0			
8	1	0.2	0.05	0.32	Fully rough
9		0.4			
10		0			
11	1	0.2	0.05	0.48	Fully rough
12		0.4			
13			0.025		
14	1	0.4	0.05	0.32	Fully rough
15			0.1		
16	1	0.4	0.05	0.32	$\mu = 0.5$

3 RESULTS

3.1 *Yield envelopes*

Figures 3-4 show the results of the finite element analysis for the cases from Table 1. The results are presented as a series of envelopes, giving the relationship between installation torque T and normal force N.

3.2 *Effect of shaft diameter*

The effect of shaft diameter d on the maximum normal force N_{max} ($T = 0$) is significant, while its effect on maximum installation torque T_{max} ($N = 0$) is negligible. The decrease in N_{max} with an increase in shaft diameter d is due to reduction in effective helix area. In Section 4.1, the relationship between N_{max} and the shaft diameter is characterized quantitatively.

3.3 *Effect of pitch and vertical force*

As can be seen from Figure 3, the shape of yield envelope is heavily dependent on the ratio of the pitch to the helix diameter, p/D. For very small pitch p, the installation torque T remains roughly constant for small values of normal force N, and then drops sharply as N increases. In other words, when the pitch is small, installation torque is largely inde-

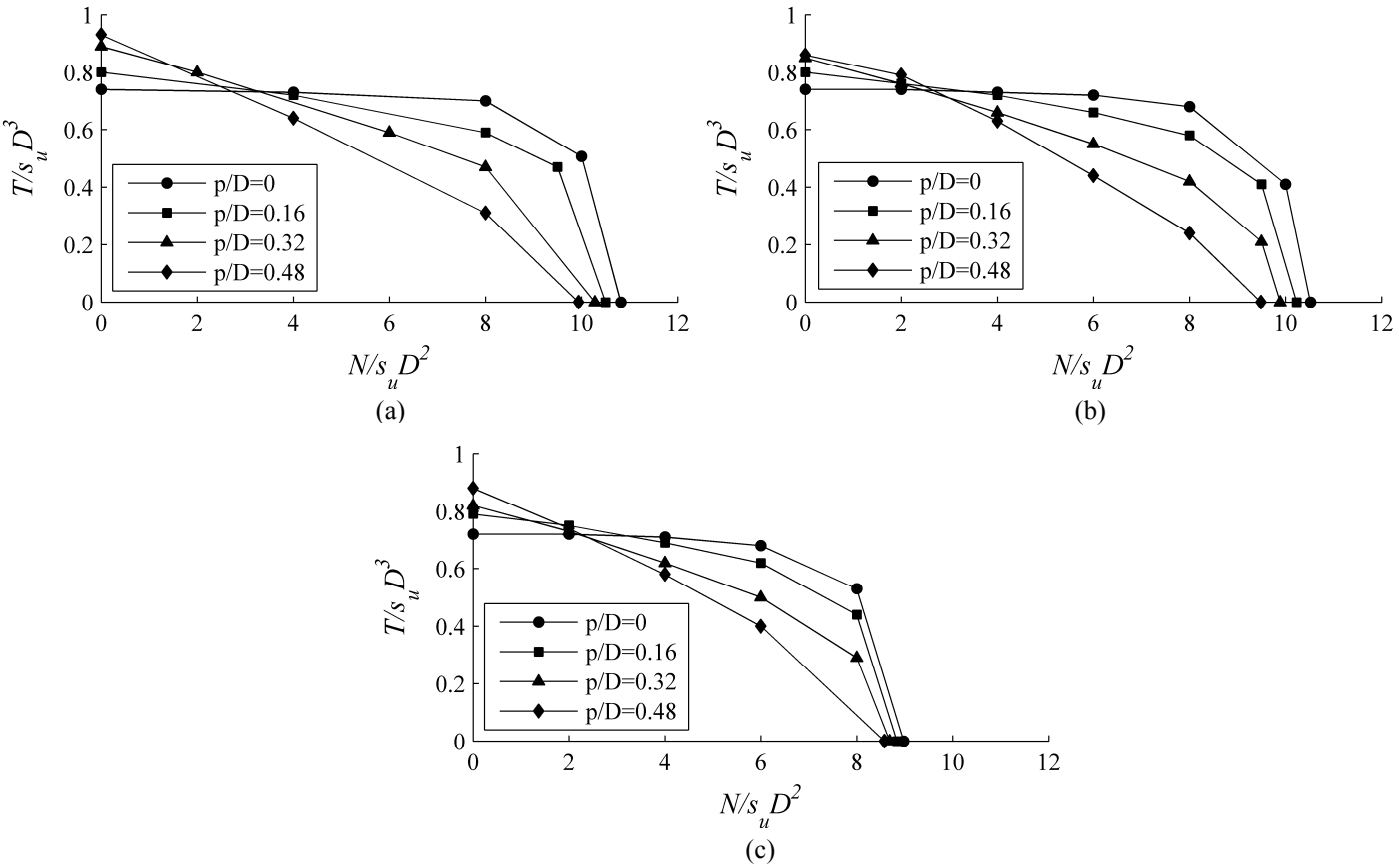

Figure 3. Normalised installation torque versus normal force: (a) $d/D = 0$, (b) $d/D = 0.2$, and (c) $d/D = 0.4$.

pendent of applied normal force. By increasing *p/D*, the slope of the yield envelope increases, and the envelope approaches a straight line. That is, the effect of vertical force becomes more significant as *p/D* grows, and *T* decreases roughly linearly with increasing *N*.

3.4 *Effect of helix thickness and roughness*

Figure 4 shows the effect of helix thickness and roughness on the yield envelope. By decreasing helix thickness or reducing friction between the soil and the helix, the yield envelope shrinks, and consequently *T* decreases.

The decrease in *T* due to a decrease in helix thickness for typical thicknesses found in industry ($0.023 \leq t/D \leq 0.086$) can be as much as 40%.

4 EXPRESSIONS FOR YIELD ENVELOPES

Methodologies for analysing the behaviour of horizontal plates assuming plain strain and undrained loading can be found in the work of Bransby and O'Neill (1999), O'Neill et al. (2003), Cassidy et al. (2012), and others. In these studies, the failure envelope for a single plate was derived assuming a local (deep) failure mechanism within the soil. That is, it was assumed that the plate has already penetrated to some depth with the soil, and the initial phase of installation was not considered. Bransby and O'Neill (1999) proposed the following yield function $f(H,V)$ describing the relationship between the tangential force H and normal force V at failure for a horizontal plate

$$f\left(H,V\right)=\left(\frac{|V|}{V_{\max}}\right)^{q}+\left(\frac{|H|}{H_{\max}}\right)^{r}-1=0 \tag{2}$$

where $V_{\max}$ and $H_{\max}$ define the capacity of the plate under purely normal loading and purely tangential loading, respectively, and exponents q and r define the shape of the yield surface. Various proposals for $V_{\max}$, $H_{\max}$, q, and r can be found, and these depend on the plate thickness, plate roughness, and the method used to determine the collapse loads.

In this study, an attempt is made to define the *T-N* yield envelopes using a formula similar to Equation (2).

4.1 *Yield envelope*

The numerical results are shown in Figure 5 together with fitted curves based on the following adaptation of Equation (2)

$$f\left(T,N\right)=\left(\frac{N}{N_{\max}}\right)^{q}+\left(\frac{T}{T_{\max}}\right)^{r}-1=0 \tag{3}$$

where N_{max} and T_{max} are maximum normal force and torque corresponding to $T = 0$ and $N = 0$, respectively. The values of N_{max} and T_{max} accounting for shaft diameter and helix pitch are approximated from the numerical results as

$$\frac{N_{\max}}{s_u D^2}=\frac{N_{\max\left(d,p=0\right)}}{s_u D^2}\left[1-\left(\frac{d}{D}\right)^2\right]\cos\beta \tag{4}$$

$$\frac{T_{\max}}{s_u D^3}=\frac{T_{\max\left(d,p=0\right)}}{s_u D^3}+0.33\frac{p}{D} \tag{5}$$

where $N_{\max(d,p=0)}$ and $T_{\max(d,p=0)}$ are for a deeply embedded circular plate and

$$\beta=\sin^{-1}\left(\frac{p}{D}\right) \tag{6}$$

The fitting parameters q, r, $N_{\max(d,p=0)}$ and $T_{\max(d,p=0)}$ are shown in Table 2. It was observed that q drops dramatically for *p/D* between 0 and 0.16 and then remains almost constant. The values given in Table 2 are therefore only valid for helices with $0.16 \leq p/D \leq 0.48$. The envelope expressed in Equations (3)-(5) pertains to helices with t/D=0.05 and fully rough conditions, although similar envelopes may be de-

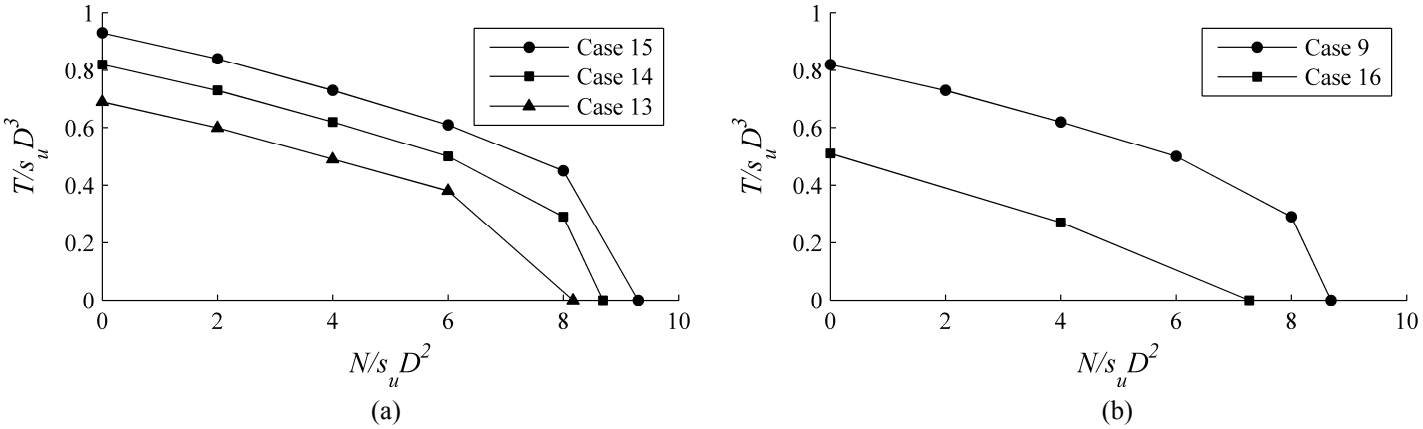

Figure 4. The effect of (a) helix thickness and (b) roughness.

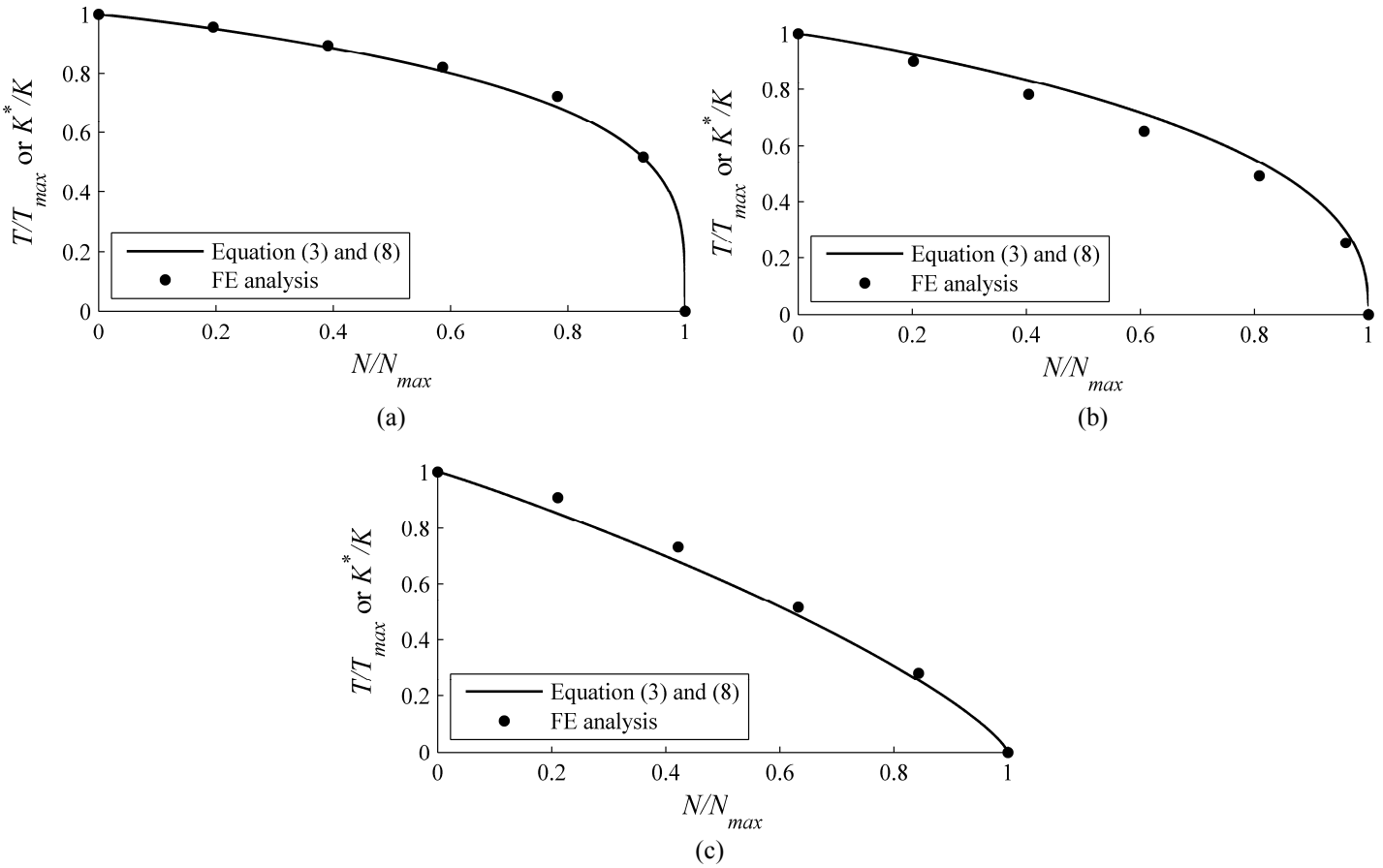

Figure 5. Comparison between yield envelopes obtained from finite element analysis and Equations (3) and (8) for (a) Case 5, (b) Case 8, and (c) Case 11.

rived for other cases.

Overall, Figure 5 reveals that the fitted envelope matches the numerical results well.

5 TORQUE-CAPACITY CORRELATION

The envelopes presented in the previous section can be directly used to relate installation torque to capacity. To demonstrate this, it should first be noted that the ultimate uplift capacity N_u in Equation (1) is identical to the maximum normal force N_{max} (corresponding to $T = 0$). This assumes that the effect of soil disturbance during installation is negligible and the anchor is deeply embedded, such that the failure mechanism is local. The torque correlation factor K can therefore be expressed as

$$K = \frac{N_{\max}}{T} \tag{7}$$

While N_{max} is constant for a particular anchor configuration, the installation torque T depends strongly on N, the normal force applied during installation. Namely, the torque T decreases as a function of N, and therefore K increases as the normal force applied during installation increases. Variations with respect to the pitch p, shaft diameter d, helix thickness t, and anchor roughness will also affect K. For example, according to the findings of this study, the normal force N applied during installation has less influence on K for anchors with small pitch as compared to those with large pitch. The installation torque T is unique and unaffected by normal force N only for $p/D = 0$ (circular plate).

A slight modification of the T-N envelope proposed in Section 4 gives the torque correlation factor

Table 2. Yield envelope curve-fitting parameters for 3D helix (this study) and rectangular plate (O'Neill et al. 2003).

Parameter	This study	O'Neill et al. (2003)
q	1.07	3.16
r	5.16-8.02(p/D)	3.41
$T_{max(d,p=0)}/s_uD^3$	0.74	-
$N_{max(d,p=0)}/s_uD^2$	10.82	-

K as follows

$$f\left(K,N\right)=\left(\frac{N}{N_{\max}}\right)^{q}+\left(\frac{K^{*}}{K}\right)^{r}-1=0 \tag{8}$$

and

$$K^{*}=\frac{N_{\max}}{T_{\max}} \tag{9}$$

where K^{*} is the torque correlation factor with no applied normal force ($N = 0$). The ratio K^{*}/K in Equation (8) is equivalent to T/T_{max} in Equation (3) by definition, and therefore the envelopes shown in Figure 5 can be used to represent either quantity.

While the torque correlation factor K depends on the normal force N applied during installation, as well as the configuration of the anchor and the soil strength, it can be observed K^{*} is independent of N. This observation may assist in appropriately contextualizing torque-capacity correlation as a field verification technique, which does not at present account for the normal force N.

6 CONCLUSIONS

In this study, a simplified approach based on small-strain finite element analysis was used to model installation of helical anchors in clay and investigate the influence of applied normal force, anchor geometry, and contact conditions on the installation torque. The approach hinges on incremental analysis of a three-dimensional helix pre-embedded at significant depth within the soil stratum, and it therefore fully captures three-dimensional effects but neglects the influence of the full history of deformation. From a practical point of view, this study modifies the conventional torque-capacity correlation method, thereby transforming an empirical method into an elegant method for assessing *in situ* soil strength and anchor capacity. Specific conclusions from this study are as follows:

1- The proposed formula for the yield envelope can predict installation torque T and normal force N applied during installation very well. However, this yield envelope is only for helices with t/D=0.05 and fully rough contact conditions. For a typical range of t/D ($0.023 \leq t/D \leq 0.086$), the yield envelope can shrink or expand up to 40%.

2- The yield envelope indicates that the normal force N applied during installation has negligible effects on installation torque for anchors with a small ratio of pitch to helix diameter (p/D), for which torque drops sharply to zero if vertical force is sufficiently large. For larger values of the pitch, on the other hand, vertical force has considerable effects on torque. This clearly suggests that vertical force and helix pitch should be taken into account in attempts to relate installation torque to uplift capacity, though such is not currently the case in practice.

3- Equations for predicting the torque-capacity correlation factor K, accounting for the vertical force, helix pitch, shaft and helix diameter, have been developed in this study. The equations reveal the significance of normal force and helix pitch on torque-capacity correlation factor.

4- Helix roughness has a significant impact on the T-N yield envelope and K factor. A smoother helix results in smaller values of installation torque T.

ACKNOWLEDGEMENT

Financial support from the Australian Research Council Centre of Excellence for Geotechnical Science and Engineering is gratefully acknowledged.

REFERENCES

Adams, J.I. & Klym, T.W. 1972. A study of anchorages for transmission tower foundations. *Canadian Geotechnical Journal* 9(1): 89–104, 10.1139/t72-007.

Bransby, M.F. & O'Neill, M. 1999. Drag anchor fluke soil interaction in clays. *Proc. 7th Int. Symp. on Numerical Models in Geomechanics*, Graz, 489–494.

Cassidy, M.J., Gaudin, C., Randolph, M.F., Wong, P.C., Wang, D., & Tian, Y. 2012. A plasticity model to assess the keying of plate anchors. *Géotechnique* 62(9): 825–836.

Merifield, R.S. 2011. Ultimate uplift capacity of multiplate helical type anchors in clay. *Journal of Geotechnical and Geoenvironmental Engineering* 137(7): 704-716.

O'Neill, M.P., Bransby, M.F., & Randolph, M.F. 2003. Drag anchor fluke–soil interaction in clays. *Canadian Geotechnical Journal* 40: 78–94.

Perko, H.A. 2000. Energy method for predicting installation torque of helical foundations and anchors, Denver, CO, USA.

Tsuha, C.H.C. & Aoki, N. 2010. Relationship between installation torque and uplift capacity of deep helical piles in sand. *Canadian Geotechnical Journal* 47(6): 635-647.

Tsuha, C.H.C., Aoki, N., Rault, G., Thorel, L., Garnier, J. 2007. Physical modelling of helical pile anchors. *International Journal of Physical Modelling in Geotechnics* 4: 1-12.

Vyazmensky, A.M. 2005. *Numerical modelling of time dependent pore pressure response induced by helical pile installation*. The University of British Columbia, Master thesis.

Wang, D., Merifield, R.S., & Gaudin, C. 2013. Uplift behaviour of helical anchors in clay. *Canadian Geotechnical Journal* 50: 575-584.

Weech, C.N. 2002. *Installation and load testing of helical piles in a sensitive fine-grained soil*. The University of British Columbia, MS Thesis.